Physics and Geometry of Flow under Curvature: Singularity Formation, Minimal Surfaces, Geodesics, and Surface Tension

James A. Sethian
Department of Mathematics
University of California
Berkeley, California 94720

David L. Chopp
Department of Mathematics
University of California
Los Angeles, California 90024

Introduction

In this paper, we study physical and geometric applications of hypersurfaces whose speed depends at least in part on the local mean curvature. The main tool is a numerical technique, introduced in [25], that accurately follows the evolving hypersurface by embedding it as the zero level set in a family of hypersurfaces. The resulting partial differential equations for the motion of the level set function may be solved by using numerical techniques borrowed from hyperbolic conservation laws. The advantage to this approach is that sharp corners and cusps are accurately tracked, and topological changes in the evolving hypersurface are handled naturally with no special attention.

This technique, known as the level set approach, is used to analyze a collection of problems. In Part One, we give the mathematical and numerical formulation for this technique. In Part Two, we discuss a collection of geometric problems. First, the collapse of a hypersurface under motion by mean curvature is studied. In [29], numerical experiments were performed of the collapse of a dumbbell, and showed that the handle pinches off and splits the single dumbbell into two separate

hypersurfaces, each of which collapses to a point. In this paper, we show that an extension of this problem produces an interesting result: a multi-armed dumbbell leaves a separate, residual closed object at the center after the singularity forms. Hypersurfaces propagating under Gaussian curvature are also considered.

Next, the level set approach is used to generate minimal surfaces attached to a one-dimensional wire frame in three space dimensions. Given a wire frame, we construct a surface passing through that 1-D curve and view it as the zero level set of a higher dimensional function. The mean curvature equation for this function is then evolved in time, producing a minimal surface as the final limiting state.

Next, we compute hypersurfaces of constant non-zero mean curvature by adding a hyperbolic component to the flow partial differential equation. As examples, catenoid-like surfaces of a variety of non-zero curvatures are computed. The extension of the level set formulation to the computation of surfaces of any prescribed function of the curvature is given.

Finally, we end our geometric examples with the generalization of the curvature flow algorithm to curves on two-dimensional manifolds in R^3. In this context, the curves flow with speed dependent on the geodesic curvature of the curve. Examples of curves on a cube, sphere, and torus are given.

In Part Three, we summarize some of the work so far in applying these level set approaches to physical problems in which motion by curvature plays a key role. Here, we provide motivation and reference for work in flame propagation, two fluid problems, crystal growth and dendritic solidification, droplet dynamics, and image reconstruction.

Part I: The Level Set Formulation

Equations of Motion

Consider a closed curve $\gamma(t)$ where t is time, $t \in [0, \infty)$, moving with speed F normal to itself. The speed F may depend on local properties of the curve such as the curvature or normal vector. The origin of the work to follow propagating interfaces began in [27,28], where the role of curvature in the speed function F for the propagating front $\gamma(t)$ was shown to be analogous to the role of viscosity in the corresponding hyperbolic conservation law for the evolving slope of $\gamma(t)$. This led to the level set formulation of the propagating interface introduced in [25]. In general terms, let $\gamma(0)$ be a closed, non-intersecting, $(N-1)$ dimensional hypersurface and construct a function $\phi(\bar{x}, t)$ defined from $R^N \times R$ to R such that the level set $\{\phi = 0\}$ is the front $\gamma(t)$, that is

$$\gamma(t) = \{\bar{x} \in R^N : \phi(\bar{x}, t) = 0\} \tag{1}$$

In order to construct such a function $\phi(\bar{x}, t)$, appropriate initial conditions $\phi(\bar{x}, 0)$ and an associated partial differential equation for the time evolution of $\phi(\bar{x}, t)$ must be supplied. We initialize ϕ by

$$\phi(\bar{x}, 0) = \pm d(\bar{x}) \tag{2}$$

where $d(\bar{x})$ is the signed distance from $\bar{x}$ to the initial front $\gamma(t = 0)$. In order to derive the partial differential equation for the time evolution of ϕ, consider the motion of some level set $\{\phi(\bar{x}, t) = C\}$. Let $\bar{x}(t)$ be the trajectory of some particle located on this level set, so that, (see [23]),

$$\phi(\bar{x}(t), t) = C \tag{3}$$

The particle velocity $\frac{\partial \bar{x}}{\partial t}$ in the direction $\bar{n}$ normal to the level set C is given by

$$\frac{\partial \bar{x}}{\partial t} \cdot \bar{n} = F. \tag{4}$$

Differentiating Eqn. (3) with respect to t and combining with Eqn. (4) yields

$$\begin{aligned} \phi_t + F\|\nabla\phi\| &= 0 \\ \phi(\bar{x}, t = 0) &= \text{given.} \end{aligned} \tag{5}$$

Eqn. (5) yields the motion of the interface $\gamma(t)$ as the level set $\phi = 0$, thus

$$\gamma(t) = \{x : \phi(\bar{x}, t) = 0\}. \tag{6}$$

Eqn. (5) is referred to as the *level set formulation*. For certain speed functions F, it reduces to some familiar equations. For example, for $F = 1$, the equation becomes the eikonal equation for a front moving with constant speed. For $F = 1 - \epsilon\kappa$, where κ is the curvature of the front, Eqn. (5) becomes a Hamilton-Jacobi equation with parabolic right-hand-side, similar to those discussed in [7]. For $F = \kappa$, Eqn. (5) reduces to the equation for mean curvature flow. When required, the curvature κ may be determined from the level set function ϕ. For example, in three space dimensions the mean curvature is given by

$$\kappa = \frac{\begin{array}{c}(\phi_{xx})(\phi_y^2 + \phi_z^2) + (\phi_{yy})(\phi_x^2 + \phi_z^2) + (\phi_{zz})(\phi_x^2 + \phi_y^2) \\ -2(\phi_x\phi_y\phi_{xy} + \phi_y\phi_z\phi_{xz} + \phi_x\phi_z\phi_{xz})\end{array}}{2(\phi_x^2 + \phi_y^2 + \phi_z^2)^{3/2}}. \tag{7}$$

There are several advantages of this approach given in Eqn. (5). First, the fixed coordinate system avoids the numerical stability problems that plague approximation techniques based on a parameterized approach. Second, topological changes are handled naturally, since the level surface $\phi = 0$ need not be simply connected. Third, the formulation clearly applies in any number of space dimensions.

To illustrate, in Figure 1 the motion of a circle in the xy-plane propagating outward with constant speed is shown. Fig. 1a shows the initial circle, while Fig. 1b shows the same circle as the level set $\phi = 0$ of the initial surface

$$\phi(x, y, t = 0) = \sqrt{x^2 + y^2} - 1.$$

The one-parameter family of moving curves $\gamma(t)$ is then matched with the one-parameter family of moving surfaces in Figs. 1c and 1d. This level set approach to front propagation has been employed in a variety of investigations, as discussed in Part Two. In some particular cases, the reaction diffusion method has also shown some promising results. The theoretical underpinnings of the level set approach have been examined in detail by Evans and Spruck [9,10]; for further theoretical work, see also [4,8,11,15].

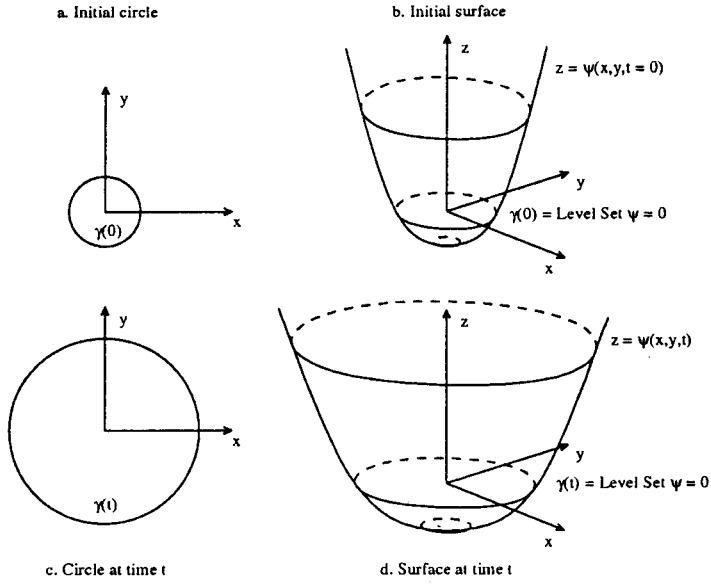

Figure 1: Eulerian formulation of equations of motion

Numerical Approximation

A successful numerical scheme to approximate Eqn. (5) hinges on the link with hyperbolic conservation laws. As motivation, consider the simple case of a moving front in two space dimensions that remains a graph as it evolves, and consider the initial front given by the graph of $f(x)$ with f, f', periodic on $[0,1]$. Let $y(x,t)$ be the height of the propagating function at time t, thus $y(x,0) = f(x)$. The normal at (x,y) is $(1,-y_x)$, and the equation of motion becomes $y_t = F(\kappa)(1+y_x^2)^{1/2}$. Using the speed function $F(\kappa) = 1 - \epsilon\kappa$, where the curvature $\kappa = y_{xx}/(1+y_x^2)^{3/2}$, we get

$$y_t - (1+y_x^2)^{1/2} = \epsilon \frac{y_{xx}}{(1+y_x^2)} \tag{8}$$

To construct an evolution equation for the slope $u = dy/dx$, we differentiate both sides of the above with respect to x and substitute to obtain

$$u_t + \left[-(1+u^2)^{1/2}\right]_x = \epsilon \left[\frac{u_x}{(1+u^2)}\right]_x \tag{9}$$

Thus, the derivative of the Hamilton-Jacobi equation with curvature-dependent right-hand-side for the changing height $y(x,t)$ is a viscous hyperbolic conservation law for the propagating slope u. With this hyperbolic conservation law, an associated entropy condition must be invoked to produce the correct weak solution beyond the development of a singularity in the evolving curvature. Complete details may be found in [29].

Considerable care must be taken in devising numerical schemes to approximate the level set Eqn. (5). Because a central difference approximation to the gradient produces the wrong weak solution, we instead exploit the technology of hyperbolic conservation laws in devising schemes which maintain sharp corners in the evolving hypersurface and choose the correct, entropy-satisfying weak solution. One of the easiest such schemes is a variation of the Engquist-Osher scheme presented in [25]. This scheme is upwind in order to follow the characteristics at boundaries of the computational domain. The scheme is as follows. Decompose the speed function F into $F = F_A + F_B$, where F_A is treated as the hyperbolic component which must be handled through upwind differencing, and the remainder F_B which is to approximated through central differencing. Let ϕ^n_{ijk} be the numerical approximation to the solution ϕ at the point $i\Delta x$, $j\Delta y$, $k\Delta z$, and at time $n\Delta t$, where Δx, Δy, Δz is the grid spacing and Δt is the time step. We can then advance from one time step to the next by means of the numerical scheme

$$\begin{aligned}\phi^{n+1}_{ij} = \phi^n_{ij} &+ F_A \Delta t \cdot \\ &\Big((\min(D^-_x \phi_{ij}, 0))^2 + (\max(D^+_x \phi_{ij}, 0))^2 + (\min(D^-_y \phi_{ij}, 0))^2 \\ &\quad + (\max(D^+_y \phi_{ij}, 0))^2 + (\min(D^-_z \phi_{ij}, 0))^2 + (\max(D^+_z \phi_{ij}, 0))^2\Big)^{1/2} \\ &+ \Delta t F_B \|\nabla \phi\|\end{aligned} \tag{10}$$

Here, the difference operators D^-_x refers to the backward difference in the x direction. The other difference operators are defined similarly.

Examples

Grayson [16] has proven that any non-intersecting closed curve in R^2 moving with speed $F(\kappa) = -\kappa$ must collapse smoothly to a circle; see also [12,13,14]. In Figure 3, is a demonstration of a closed spiral curve shrinking towards a circle. Note that the calculation follows a family of spirals lying on the higher dimensional surface. The particular front corresponding to the propagating curve vanishes when the evolving surface moves entirely above the xy-plane, that is, when $\phi(x,y,t) > 0$ for all (x,y).

As a different example, let the wound spiral in the previous example represent the boundary of a flame burning with speed $F(\kappa) = 1 - \epsilon\kappa$, $\epsilon = 0.1$. Here, the entropy condition is needed to account for the change in topology as the front burns together. In Fig. 4a, the initial spiral as the boundary of the shaded region is given. In Fig. 4b, the spiral expands, and pinches off due to the outward normal burning and separates into two flames, one propagating outward and one burning in. In Figure 4c, the front is the boundary of the shaded region. The outer front expands and the inner front collapses and disappears. In Fig. 4d all that remains is the outer front which asymptotically approaches a circle.

Part II: Geometric Problems in Curvature Flow

Collapsing Dumbbells under Mean Curvature Flow

In this section, singularity formation of hypersurfaces in three space dimensions propagating under mean curvature is studied. Theoretical discussion of such flows have been made in [3,17,20]. Numerical calculations based on a marker Lagrangian approach have been made in [2].

A well-known example is the collapse of a dumbbell, studied numerically in [27], and theoretically in [18,21]. In Fig. 2, the cross-section of the evolution of a dumbbell collapsing under its mean curvature ($F(\kappa) = -\kappa$) is given. In Figure 2a, various time snapshots of the collapsing dumbbell are shown. As can be seen from the evolving shape, the center handle of the dumbbell pinches off, separating the collapsing hypersurface into two pieces.

A more complicated version is shown in Figure 5, which shows the collapse of a four-armed dumbbell. Four different singularities form leaving a residual pillow in the center which collapses smoothly through a spherical shape to a point.

As a final demonstration of this process, Figures 6 and 7 show the collapse of a diagonal lattice of tubes. The lattice shown in Figure 6a (Time = 0.0) has periodic boundary conditions; thus, the figure represents one section of an infinite lattice. As the hypersurface collapses, the pillow emerges at the intersection of the tubes. A wholly different result is shown in Figure 7, where the same tube lattice is shown, only this time with thicker tubes (Figure 7a). In this case, the separate pillows appear in the *holes* of the lattice, as the evolving surface collapses around them.

Next, a three-dimensional version of the spiral collapsing under mean curvature is computed. The three-dimensional spiral hypersurface shown in Figure 8 is actually hollow on the inside; the opening on the right end extends all the way through the object to the leftmost tip. As the hypersurface collapses under its mean curvature, the inner sleeve shrinks faster than the outer sleeve, and withdraws to the rightmost edge before the outer sleeve collapses around it.

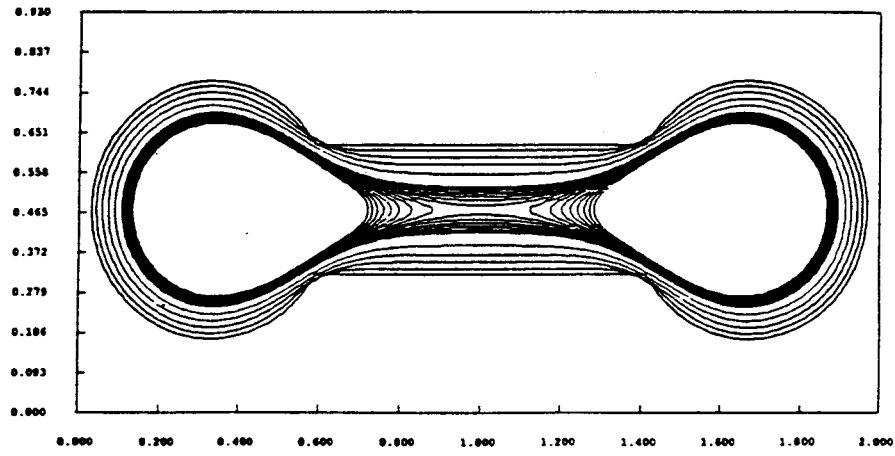

Figure 2: Collapsing Dumbbell

Collapsing Surfaces under Gaussian Curvature Flow

A variation on the above study can be performed using Gaussian curvature instead of mean curvature. Starting with the definition of Gaussian curvature κ_{Gaussian} for a surface (see [19]), an expression for κ_{Gaussian} in terms of the level set function ϕ can be obtained, namely

$$\kappa_{\text{Gaussian}} = \frac{\begin{array}{c}\phi_x^2(\phi_{yy}\phi_{zz} - \phi_{yz}^2) + \phi_y^2(\phi_{xx}\phi_{zz} - \phi_{xz}^2) + \phi_z^2(\phi_{xx}\phi_{yy} - \phi_{xy}^2) \\ - 2[\phi_x\phi_y(\phi_{xz}\phi_{yz} - \phi_{xy}\phi_{zz}) + \phi_y\phi_z(\phi_{xy}\phi_{xz} - \phi_{yz}\phi_{xx}) \\ + \phi_x\phi_z(\phi_{xy}\phi_{yz} - \phi_{xz}\phi_{yy})]\end{array}}{(\phi_z^2 + \phi_y^2 + \phi_x^2)^2}. \quad (11)$$

Suppose we consider flow of surfaces under Gaussian curvature. If the closed hypersurface is convex, the Gaussian curvature will not change sign, and the surface should collapse as it flows, see [24]. In Figure 9, the motion of a flat disk-like surface collapsing under its Gaussian curvature is shown. The sharply curved regions move in quickly, since they are regions of high Gaussian curvature, and the hypersurface moves towards a spheroidal shape.

In the case of non-convex closed hypersurfaces, the problem acts like the backwards heat equation due to the fact that Gaussian curvature is the *product* of the two principle curvatures. Thus, non-convex hypersurfaces go unstable in most cases as shown in Figure 10.

Construction of Minimal Surfaces

In this section, the level set perspective is used to construct minimal surfaces. Consider a closed curve $\Gamma(s)$ in R^3; $\Gamma : [0,1] \rightarrow R^3$. The goal is to construct a membrane with boundary Γ and mean curvature zero.

Given the bounding wire frame Γ, consider some initial surface $S(t=0)$ whose boundary is Γ. Let $S(t)$ be the family of surfaces parameterized by t obtained by allowing the initial surface $S(t=0)$ to evolve under mean curvature, with boundary given by Γ. Defining the surface S by $S = \lim_{t\rightarrow\infty} S(t)$, one expects that the surface S will be a minimal surface for the boundary Γ. Thus, given an initial surface $S(0)$ passing through Γ, construct a family of neighboring surfaces by viewing $S(0)$ as the zero level set of some function ϕ over all of R^3. Using the level set Eqn. (5), evolve ϕ according to the speed law $F(\kappa) = -\kappa$. Then the minimal surface S will be given by

$$S = \lim_{t\rightarrow\infty} \{\bar{x} : \phi(\bar{x}, t) = 0\}. \tag{12}$$

The difficult challenge with the above approach is to ensure that the evolving zero level set always remains attached to the boundary Γ. This is accomplished by creating a set of boundary conditions on those grid points closest to the wire frame and link together the neighboring values of ϕ to force the level set $\phi = 0$ through Γ. The details for this construction can be found in Chopp [5].

As a test example, the minimal surface spanning two rings has an exact solution given by the catenoid

$$r(x) = a\cosh(x/a) \tag{13}$$

where $r(x)$ is the radius of the catenoid at a point x along the x axis, and a is the radius of the catenoid at the center point $x = 0$. In Figure 11, the minimal surface spanning two rings each of radius 0.5 and at positions $x = \pm.277259$ is computed. A cylinder spanning the two rings is taken as the initial level set $\phi = 0$. Next, in Figure 12, this same problem is computed, but the rings are placed far enough apart so that a catenoid solution cannot exist. As the surface evolves, the middle pinches off and the surface splits into two surfaces, each of which quickly collapses into a disk. The final shape of a disk spanning each ring is indeed a minimal surface for this problem.

This example illustrates one of the virtues of the level set approach. No special cutting or *ad hoc* decisions are employed to decide when to break the surface. Instead the characterization of the zero level set as but one member of a family of flowing surfaces allows this smooth transition. More complex examples of minimal surfaces are given in [6].

Surfaces of Constant Mean Curvature

The above technique can be extended to produce surfaces of constant but non-zero mean curvature. In order to construct a surface of constant curvature κ_0,

start with any initial surface passing through the initial wire frame and allow it to propagate with speed

$$F(\kappa) = \kappa_0 - \kappa. \tag{14}$$

Here, the "constant advection term" κ_0 is taken as the hyperbolic component F_A, and treated using the entropy-satisfying upwind difference solver, while the parabolic term κ is taken as F_B, and is approximated using central differences.

Using the two ring "catenoid" problem as a guide, in Figure 13 this technique is used to compute the surface of constant curvature spanning the two rings. In each case, the initial shape is the cylinder spanned by the rings. The final computed shapes for a variety of different mean curvatures are shown.

Surfaces of Non-Constant Mean Curvature

Finally, this technique is extended to allow the calculation of surfaces of a prescribed function of the curvature. Suppose we wish to find a surface of curvature $A(\bar{x})$ passing through a given wire frame, where A is some given function of a point $\bar{x}$ in three-dimensional space. Using the above approach, the initial bounded zero level surface is evolved with speed

$$F(\kappa) = A(\bar{x}) - \kappa. \tag{15}$$

As a simple example, the surface spanning two rings with curvature at any point x along the x-axis given by $10\cos(10x)$ is constructed. The obtained wavy surface with prescribed curvature is shown in Figure 14d. The rings are located at ± 0.305, with radius 0.5.

Geodesic Curvature Flow

The curvature flow algorithm can be generalized to other two-dimensional spaces. For example, we may let the level set function ϕ be defined on a two-dimensional differentiable manifold in R^3 with speed depending on geodesic curvature. The fixed boundary condition techniques for minimal surfaces can also be applied here. In this case, a curve with fixed endpoints should flow towards a geodesic of the manifold, i.e. a curve with constant geodesic curvature zero.

We begin the examples of geodesic curvature flow with flow on a sphere. The gap in Figure 15 shows the boundary of the domain, the function is assumed to be periodic across the gap. Figure 15 shows an initial circle just smaller than a great circle shrinking to a point at the top.

Figure 16 shows a single curve flowing on a torus. In order to implement the level set method on this surface, the computations must be done on a collection of coordinate patches. For the full details of how coordinate patches are used and connected, see Chopp [5].

Another example of flow on a submanifold is when the manifold is thaway from the center over a ridge.

Finally, in Figures 18, 19, we show flows on a cube. The cube is constructed with six coordinate patches corresponding to the faces of the cube. Additional examples can be found in [5].

Part III. Physical Applications

In this part, we discuss several physical problems that have been analyzed using the above level set technique.

Flame Propagation

The original motivation for our use of a level set approach arose from problems in flame propagation and combustion, where the propagating flame front can become extremely convoluted, due to cusping and wrinkling. The dynamics of a burning front are complex, depending in part on vorticity released at the front whose strength depends on the local curvature at the interface. A level set approach is well-suited to such problems, since the accurate determination of the curvature can be used to generate the proper amount of flame-induced vorticity. Here, the basic idea is to use an idealized model of combustion and view the flame as an infinitely thin front across which the reactants undergo a single step irreversible on by means of a second-order finite difference projection scheme for fluid mechanics. A random vortex method is coupled to the level set technique in [26] to study the dynamics of a flame attached to a flame holder in confined channel. The full effects of exothermicity and vorticty-production are analyzed, showing wrinkling, cusping, and the development of flame brushes as a function of turbulence levels.

Two Fluid Problems

Another fluid dynamic application of the level set approach was performed in [23]. Here, the level set technique was used to track the boundary between two different fluids in the Rayleigh-Taylor instability. Analysis of two different approaches was done; one in which the level set equation was solved directly, and one in which a conservative form of the equation was incorporated into the other four conservation laws. Results show the development of large convective rolls and the effects of viscosity on the instabilities in the flow.

Crystal Growth and Dendritic Solidification

In [30], the level set approach was applied to computing the motion of dendritic boundaries in unstable solidification. The motivation here was the ability of the level set approach to accurately compute the curvature which is required in the evaluation of the correct jump conditions across the solid/liquid interface.

The physical motivation for the problem is as follows. Begin with a supercooled liquid in a box. Under certain conditions, a seed of frozen material placed in the bath will grow in an unstable manner as the boundary freezes, producing complex shapes such as those produced in snowflakes. One model of this growth assumes the heat equation in both the solid and liquid phases, together with a set of jump conditions across the interface which determine the normal velocity of the interface in terms of the temperature and the local curvature.

The application of the level set approach to this problem begins with a boundary integral formulation of the problem due to Strain. This boundary integral formulation gives the normal velocity of the interface in terms of the current and past positions of the interface. The central idea is to view the boundary as the zero level set of the level set function, and to then extend the boundary integral formulation to provide a velocity field throughout the entire domain. This extension velocity field is then used to move all the level sets and thus update the position of the freezing boundary. For details, see [30].

Using this technique, the motion of dendritic boundaries under such effects as heat release, kinetic effects, crystalline anisotropy, initial shape, and undercooling are considered. Results show a variety of physical phenomena, including tip splitting, side growth, cusping, and morphological changes. A complete description of this algorithm and the results may be found in [30].

Droplet Dynamics

An application currently under way links the level set technique to a projection method in order to study the dynamics of a droplet falling into a bath. Here, the local curvature determines the surface tension which is responsible for the "crown"-like structure that develops in the splash. The two-dimensional results show the change of topology as the falling droplet merges with the still bath, and the resulting symmetric spiking of the fluid into the air. A three-dimensional simulation is underway. For details, see [1].

Image Processing

A different application of a level set approach is in the area of edge detection in bitmap images. Here, the main idea is extract from a pixel map the location of the edges of a potentially complex collection of boundaries. In [22] level set

schemes are merged with propagating snake techniques to produce an algorithm which robustly identifies images in tomographic scans and density maps.

Acknowledgments: The first author was supported in part by the Applied Mathematics Subprogram of the Office of Energy Research under contract DE–AC03–76SF00098, and the National Science Foundation and DARPA under grant DMS–8919074. The second author was supported in part by the National Science Foundation under grant CTS–9021021. A video (VHS format) of the evolving surfaces is available from the first author. All calculations were performed at the University of California at Berkeley and the Lawrence Berkeley Laboratory. The figures were computed using the facilities of the Graphics Group at the Lawrence Berkeley Laboratory. We would like to thank L. Craig Evans, F.A. Grunbaum, Ole Hald, and V. Oliker for helpful discussions.

References

[1] A. Bourlioux and J. A. Sethian Two and Three Dimensional Droplet Dynamics. to be submitted for publication, 1993.

[2] K. A. Brakke. *The Motion of a Surface By Its Mean Curvature.* Princeton University Press, Princeton, New Jersey, 1978.

[3] K. A. Brakke. Surface evolver program. Research Report GCG 17, the Geometry Supercomputer Project, 1200 Washington Ave. South, Minneapolis, MN 55455, 1990.

[4] Y. Chen, Y. Giga, and S. Goto. Uniqueness and existence of viscosity solutions of generalized mean curvature flow equations. *Journal of Differential Geometry*, 33:749–786, 1991.

[5] D. L. Chopp. Flow under geodesic curvature. Technical Report CAM 92-23, UCLA, May 1992.

[6] D. L. Chopp. Computing minimal surfaces via level set curvature flow. *Journal of Computational Physics*, to appear.

[7] M. G. Crandall and P. L. Lions. Viscosity solutions of Hamilton-Jacobi equations. *Transactions of the American Mathematical Society*, 277(1), 1983.

[8] L. C. Evans, H. M. Soner, and P. E. Souganidis. Phase transitions and generalized motion by mean curvature. *Communications on Pure and Applied Mathematics*, 45(9):1097–1123, 1992.

[9] L. C. Evans and J. Spruck. Motion of level sets by mean curvature I. *Journal of Differential Geometry*, 33:635–681, 1991.

[10] L. C. Evans and J. Spruck. Motion of level sets by mean curvature II. *Transactions of the American Mathematical Society*, 330:321–332, 1992.

[11] M. Falcone, T. Giorgi, and P. Loretti. Level sets of viscosity solutions and applications. Technical report, Instituto per le Applicazioni del Calcolo, Rome, 1990. preprint.

[12] M. Gage. An isoperimetric inequality with applications to curve shortening. *Duke Math Journal*, 50(1225), 1983.

[13] M. Gage. Curve shortening makes convex curves circular. *Inventiones Mathematica*, 76(357), 1984.

[14] M. Gage and R. S. Hamilton. The equation shrinking convex planes curves. *Journal of Differential Geometry*, 23(69), 1986.

[15] Y. Giga and S. Goto. Motion of hypersurfaces and geometric equations. *Journal of the Mathematical Society*, to appear.

[16] M. Grayson. The heat equation shrinks embedded plane curves to round points. *Journal of Differential Geometry*, 26(285), 1987.

[17] M. Grayson. A short note on the evolution of surfaces via mean curvature. *Duke Mathematical Journal*, 58:555–558, 1989.

[18] M. Grayson. Shortening embedded curves. *Journal of Differential Geometry*, 129:71-111, 1989.

[19] N. J. Hicks. *Notes on Differential Geometry*. Van Nostrand, Princeton, NJ, 1965.

[20] G. Huisken. Flow by mean curvature of convex surfaces into spheres. *Journal of Differential Geometry*, 20(237), 1984.

[21] G. Huisken. Asymptotic behavior for singularities of the mean curvature flow. *To appear, Journal of Differential Geometry*. .

[22] R. Malladi and J. A Sethian. Edge detection and Propagating Interface Techniques. Center for Pure and Applied Mathematics Technical Report, 1993.

[23] W. Mulder, S. Osher, and J. A. Sethian. Computing interface motion in compressible gas dynamics. *Journal of Computational Physics*, 100(2):209–228, 1992.

[24] V. Oliker. Evolution of nonparametric surfaces with speed depending on curvature, I. the Gauss curvature case. preprint, 1991.

[25] S. Osher and J. A. Sethian. Fronts propagating with curvature-dependent speed: Algorithms based on Hamilton-Jacobi formulations. *Journal of Computational Physics*, 79(1), November 1988.

[26] C. Rhee, L. Talbot, and J. A, Sethian. A Level Set Approach to Flame Propagation. Submitted for publication, Combustion and Flame, 1993.

[27] J. A. Sethian. Curvature and the evolution of fronts. *Communications in Mathematical Physics*, 101:487–499, 1985.

[28] J. A. Sethian. Numerical methods for propagating fronts. In P. Concus and R. Finn, editors, *Variational Methods for Free Surface Interfaces*. Springer-Verlag, New York, 1987.

[29] J. A. Sethian. A review of recent numerical algorithms for hypersurfaces moving with curvature-dependent speed. *Journal of Differential Geometry*, 31:131–161, 1989.

[30] J. A. Sethian and J. Strain. Crystal growth and dendrite solidification. *Journal of Computational Physics*, 98(2):231–253, 1992.

[31] J. Zhu and J. A. Sethian. Projection methods coupled to level set interface techniques. *Journal of Computational Physics*, 102(1):128–138, 1991.

Figure 3: Collapsing 2-dimensional spiral

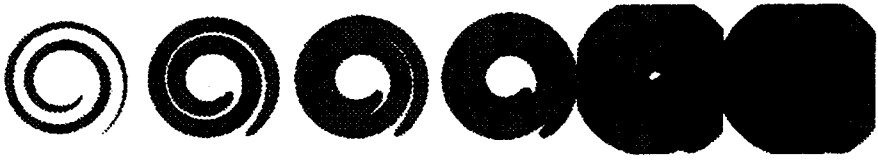

Figure 4: Burning spiral

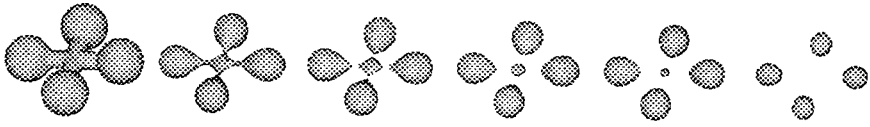

Figure 5: Collapse of a four-armed dumbbell

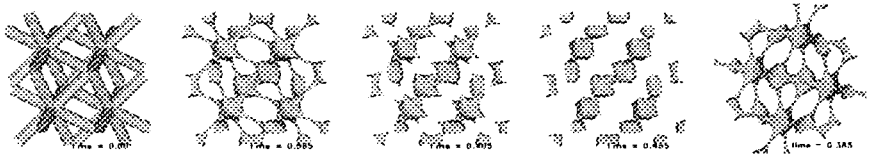

Figure 6: Collapse of a periodic lattice, small tubes

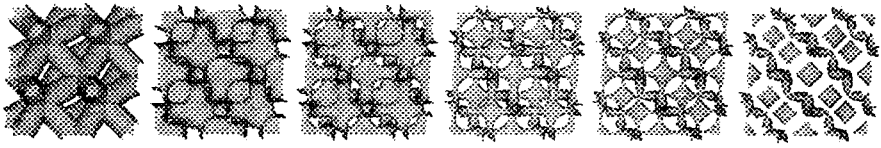

Figure 7: Collapse of a periodic lattice, large tubes

Figure 8: Collapse of a twisted test tube

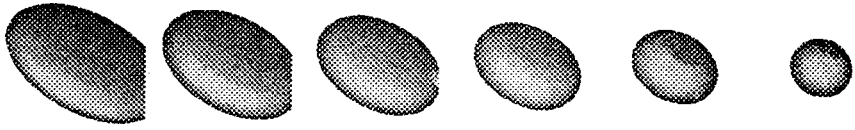

Figure 9: Collapse of a surface under Gaussian curvature

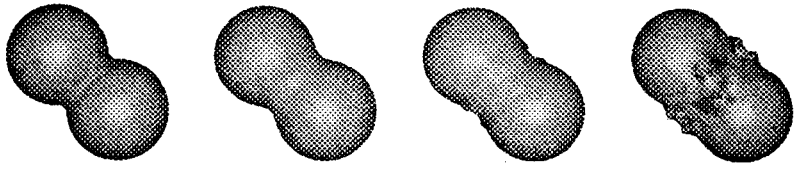

Figure 10: Collapse of a non-convex surface under Gaussian curvature

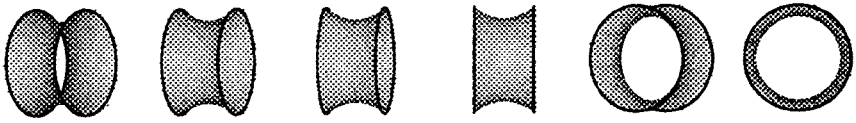

Figure 11: Euler's catenoid minimal surface

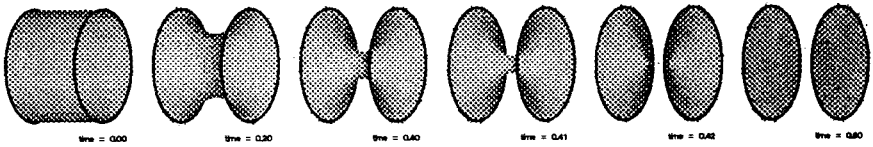

Figure 12: Splitting catenoid evolution

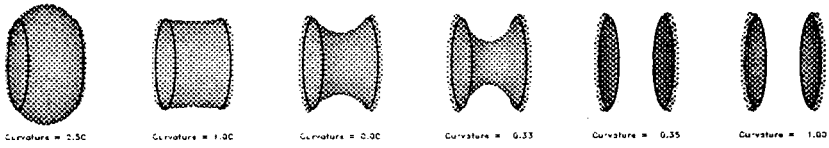

Figure 13: Constant mean curvature surfaces with fixed boundary

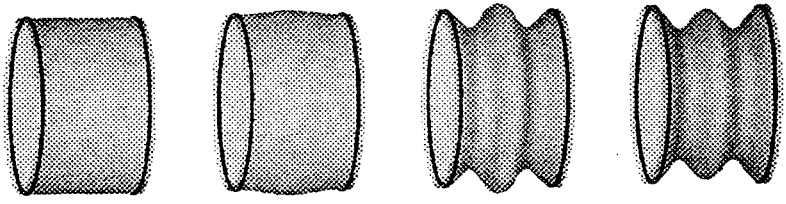

Figure 14: Non-constant prescribed curvature surface

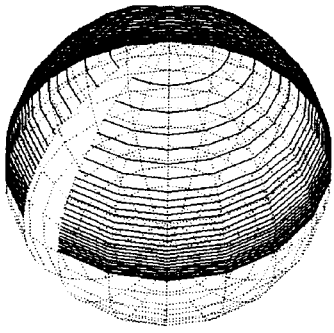

Figure 15: Circle shrinking on a sphere

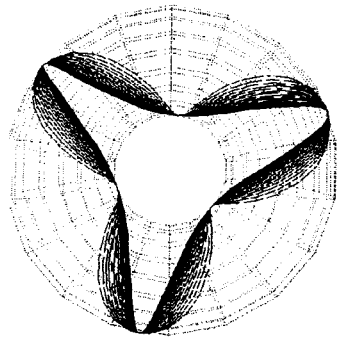

Figure 16: A single curve flowing on a torus

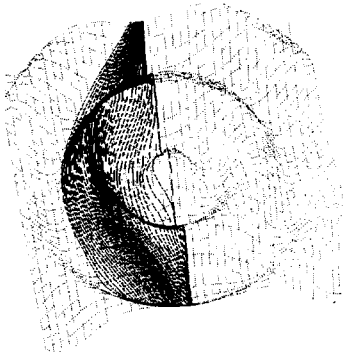

Figure 17: A curve flowing on the graph of $f(x,y) = 2\cos(2\sqrt{x^2+y^2})$

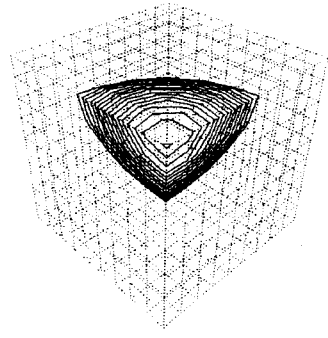

Figure 18: A single loop flowing on a cube with orthogonal edges

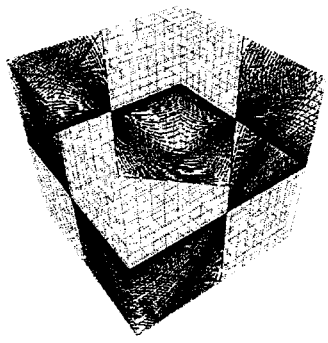

Figure 19: A single loop pulled over alternating corners